Federation University ResearchOnline

https://researchonline.federation.edu.au

Copyright Notice

This is the published version of:

Munir, N., Awrangjeb, M., Stantic, B., Lu, G., and Islam, S.: Voxel-based extraction of individual pylons and wires from lidar point cloud data, ISPRS Ann. Photogramm. Remote Sens. Spatial Inf. Sci., IV-4/W8, 91–98, 2019.

Available online at: https://doi.org/10.5194/isprs-annals-IV-4-W8-91-2019

See this record in Federation ResearchOnline at:
http://researchonline.federation.edu.au/vital/access/HandleResolver/1959.17/180873

VOXEL-BASED EXTRACTION OF INDIVIDUAL PYLONS AND WIRES FROM LIDAR POINT CLOUD DATA

N. Munir[1]*, M. Awrangjeb[1], B. Stantic[1], G. Lu[2], S. Islam[2]

[1] School of Information and Communication Technology, Griffith University, QLD 4111, Australia -@nosheen.munir@griffithuni.edu.au
[2] School of Science, Engineering and Information Technology, Federation University, QLD 4000, Australia - guojun.lu@federation.edu.au

Commission VI, WG VI/10

KEY WORDS: LiDAR, Extraction, Power line corridor, wires, SVM, pylon

ABSTRACT:

Extraction of individual pylons and wires is important for modelling of 3D objects in a power line corridor (PLC) map. However, the existing methods mostly classify points into distinct classes like pylons and wires, but hardly into individual pylons or wires. The proposed method extracts standalone pylons, vegetation and wires from LiDAR data. The extraction of individual objects is needed for a detailed PLC mapping. The proposed approach starts off with the separation of ground and non ground points. The non-ground points are then classified into vertical (e.g., pylons and vegetation) and non-vertical (e.g., wires) object points using the vertical profile feature (VPF) through the binary support vector machine (SVM) classifier. Individual pylons and vegetation are then separated using their shape and area properties. The locations of pylons are further used to extract the span points between two successive pylons. Finally, span points are voxelised and alignment properties of wires in the voxel grid is used to extract individual wires points. The results are evaluated on dataset which has multiple spans with bundled wires in each span. The evaluation results show that the proposed method and features are very effective for extraction of individual wires, pylons and vegetation with 99% correctness and 98% completeness.

1. INTRODUCTION

In the past few years assessment and monitoring of power line corridor (PLC) is gaining importance and has become an area of active research. The conventional methods for inspection of electric network rely on the participation of ground personnel and airborne camera to patrol power lines (PLs) and have limitations such as need of intensive labour and low efficiency. Remote sensors such as optical images, synthetic aperture radar (SAR) images and airborne laser Sacanner (ALS) data for PLC monitoring is part of an active research now a days. To date, optical and SAR images are commonly used to extract PLC objects. But these sensors have limitations such as weather dependency and occlusion. Airborne light detection and ranging (LiDAR) has been proven a powerful tool to overcome these limitations to enable more efficient inspection. A detailed survey on PLC monitoring methods is given in (Matikainen et al., 2016).

Majority of the studies in literature has focused on extraction and classification of pylons, wires and vegetation points as whole, less concentration has been given in extraction of individual object points which is very important for 3D modelling. Therefore, the goal of this paper is to focus on extraction of individual PLC key objects i.e., wires, pylons and trees.

2. RELATED WORK

In the literature, the PL object extraction methods based on point clouds fall to two main classes: supervised and unsupervised classification methods. The unsupervised methods generally employ statistical analysis and pattern

recognition techniques like the Hough transform (HT) and RANdom SAmple Consensus (RANSAC) to extract PL objects. Axelsson (Axelsson, 1999) proposed a classification algorithm based on the minimum descriptor length criterion using the laser reflectance data and multiple echoes. The classification results were refined by using HT algorithm in the 2D grid space. The iterative HT was applied on the grid data in (Melzer and Briese, 2004) to extract lines and clustered them together to get positions of pylons. Zhu and Hyyppä (Zhu, 2014) used statistical analysis of height, intensity and histogram analysis to detect PL points and performed a shape-based analysis to separate PLs from other objects. A voxel-based piecewise line detection technique was proposed by (Jwa et al., 2009) to group PL points in fragments and to reconstruct them using catenary curve equation. These unsupervised methods provide high level of automation, but certain assumptions are based on geometric and radiometric characteristics of point cloud, therefore the classification rules are hard to transfer from a point cloud to another.

As for the supervised classification, (McLaughlin, 2006) used the Guassian mixture model to extract transmission lines (TLs) from airborne LiDAR data. Sohn et al. (Sohn et al., 2012) used the Markov Random Field (MRF) classifier to separate objects with linear and planner features. Then, the linear features not representing wires were converted into 2D grid and the Random Forests (RF) classifier was applied to detect pylons. Finally, the RANSAC was applied on the PL candidates to form line segments. Kim and Sohn (Kim and Sohn, 2011) computed 21 features using voxel- and sphere-based neighbourhoods and used the RF to categorise data into five classes : grounds, vegetations, pylons, wires and buildings. Kim and Sohn (Kim and Sohn, 2010) used point-based and voxel-based features to classify PL objects using RF classifier. Guo et al. (Guo et al., 2015) used the JointBoost classifier with geometric features to

---

*Corresponding author

classify PL scene and optimise the results using a graph-cut segmentation method. Wang et al. (Wang et al., 2017) proposed a semi-automated PL classification method constructing PLC direction using the HT with RANSAC algorithms and applied the Support Vector Machine (SVM) classifier to classify PL points using a slanted cylindrical neighbourhood.

The supervised classification-based methods require large training datasets which are hard to collect for desired results and an unbalanced sampling in the training set increases the rate of misclassification. The reason is that pylons and wires are minor classes in any scene. For example, the dataset used in (Kim , Sohn) had only 0.81% points for pylons. The use of unbalanced classes of data gives inaccurate results. Moreover, most of the previous classification methods described the extracted PL objects as whole classes and less attention has been given to extraction of individual wires, pylons and vegetation.

The main objective of the proposed method is to extract standalone pylons, vegetation and wires from LiDAR data using supervised and unsupervised methods. While the methods in literature were more focused on classification of points as whole class and did not extracted the wires individually from complete corridor. The supervised method is employed initially by using support vector machine (SVM) classifier to separate vertical and non vertical points by through vertical profile features (VPF). From the non ground points, individual pylons and vegetation are extracted using their shape and area properties. The PL is made up of multiple spans. The location of two successive pylons are used to extract span points between them. The span points are further divided in to individual wire points by using the alignment properties of wires in a 3D voxel grid.

The remainder of this paper is structured as follows. Section III describes the proposed method in detail. Section IV presents the experimental setup with results and discussions for evaluation of the proposed method. Finally, conclusion is presented with a brief on future research directions in Section V.

3. PROPOSED METHOD

Figure 1 illustrates the work flow of the proposed method. The steps in red rectangle are for pylon and vegetation extraction while the steps in blue rectangle belong to wire extraction.

First, the input points are divided into ground and non-ground points, while the later contains objects such as pylons, wires and vegetation. The non-ground points are then classified into vertical (e.g., pylons and vegetation) and non-vertical (e.g., wires) object points using the VPF through the binary SVM classifier. A binary mask is generated from the vertical object points, from where individual pylons and vegetation are extracted by using their shape and area properties. For extraction of wires, individual span points are first extracted between the pylon locations. Then, points in each span are used to extract the individual wires by using their alignment property in voxels. Finally, the wire segments are concatenated to get each individual wire in corridor. Figure 2(a) shows a sample scene of 517 m long from the test dataset and it will be used to describe the steps of the proposed method.
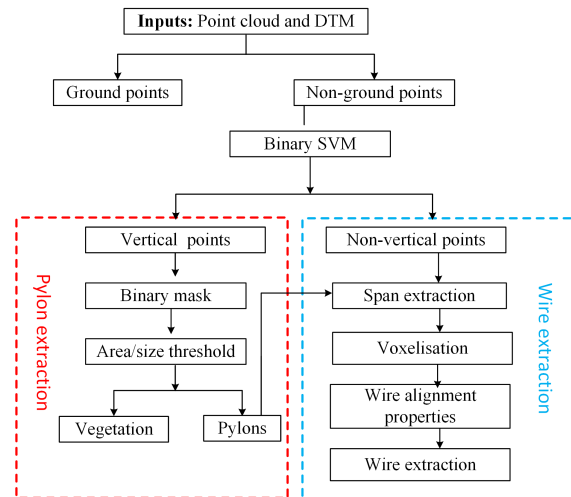

Figure 1. The work flow of the proposed method.

3.1 Extraction of Pylons and Vegetation

Usually a height of 1 m (Awrangjeb et al., 2017) is added to the local digital terrain model (DTM) height to separate the non-ground points from the rest, which contains points from the ground and the low height vegetation. Although the DTM can be generated from the LiDAR data, we assume it is available with the data. If not available, it can be generated by using software like MARS Explorer (, n.d.). The non-ground points, as shown in Figure 2(b), are expected to contain only the objects of interest, such as pylons and wires in this case. However, the test dataset has a moderate high vegetation (trees). Pylons and trees in the data show vertical continuity, while wires hang over the terrain surface and, thus, show vertical discontinuity. By exploiting this property, the VPF are extracted by using the method described in (Kim , Sohn), where voxel grids of 5 m $\times$ 5 m $\times$ 5 m are generated over the test area and each voxel is divided into fixed segments of 1 m height. The number of "continuous on segments" C_n and the number of "continuous off segments" C_f are computed for each voxel. While wires show low value for C_n but high value for C_f, vegetation and pylons display the opposite. Thereafter, the supervised SVM classifier is used to divide the LiDAR points into two sets: vertical and non-vertical points. Figures 2(c) and (d) illustrate the vertical and non-vertical points, respectively, for the sample scene.

The vertical points include pylons and trees. For separation of these objects a binary mask M, shown in Figure 2(e), is generated using the method described in (Awrangjeb et al., 2017). The resolution of M is set fixed at 0·25 m (Awrangjeb et al., 2017) and all pixels are initially filled with 1 (white). Then, for each non-ground point within a pixel, a neighbourhood (e.g., 3×3, consistent with the point density) is filled with 0 (black). Due to random and sparsity properties of the input LiDAR data, M is flood filled to remove holes. In Figure 2(e) a magnified version of a few objects are shown before and after the filling.

A connected component analysis is carried out on the filled image to obtain individual object boundaries. Assuming the maximum length or width of a pylon is 10 m, an area threshold $T_a = 100$ m^2 (Awrangjeb et al., 2017) is applied to remove trees with large horizontal areas. For each surviving connected component, all the non-ground points P_b within its boundary
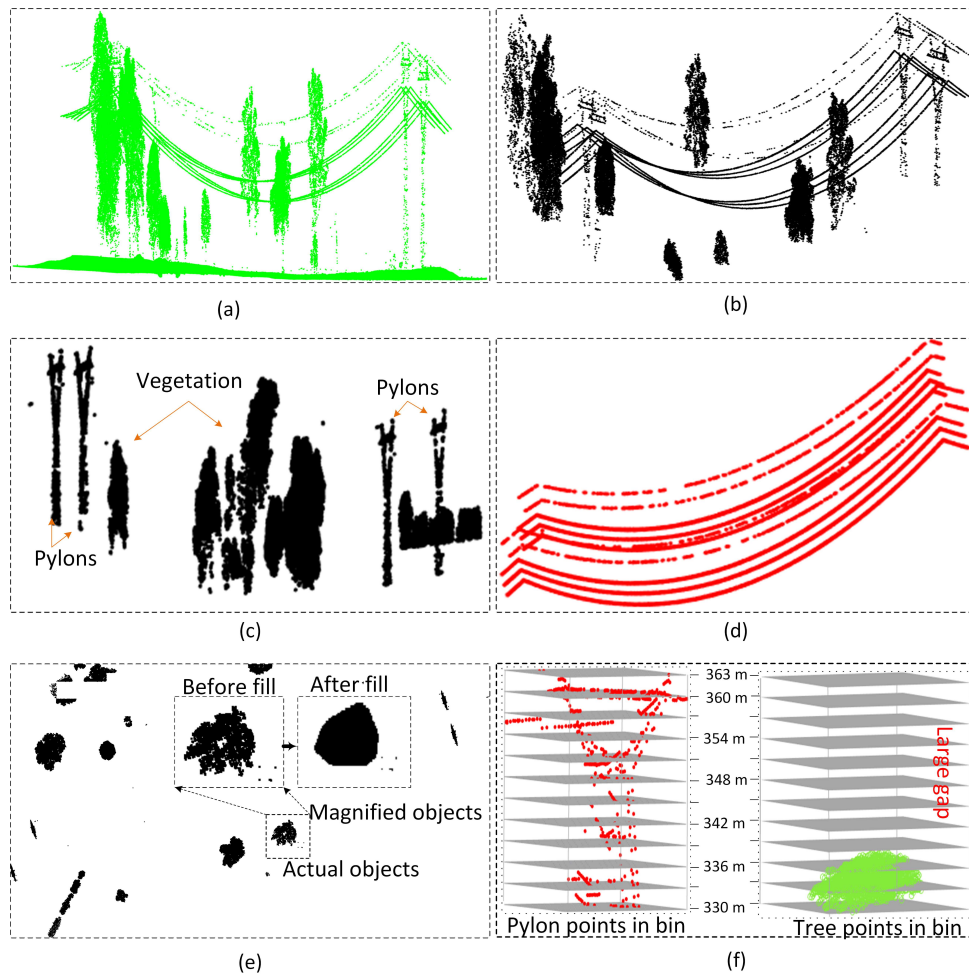
Figure 2. (a) A sample scene, (b) Non-ground points, (c) Vertical object points, (d) Non-vertical object points, (e) Binary mask, and (f) Height bins for points of a pylon and a tree.

are taken and a 3D cuboid is formed based on the minimum and maximum Easting (x), Northing (y), and Height (z) values, where x and y values are estimated from P_b, but z values are from the dataset.

These values are based on the fact that pylons reach the maximum heights of the wires attached to them, while trees usually do not reach these maximum heights. Therefore, for a vegetation there is a huge gap towards the top of the cuboid, but for a pylon there is no, or a little gap exists at the top (see Figure 2(f)). The cuboid is then divided into bins b_n, where $n \geq 1$, in the height direction. The value of n is empirically set to be 12 based on the input point density. While for a smaller value of n there may be many bins exist without any points from the top to bottom of a pylon, for a larger value of n there may be no bins exist without any points of a tree. The number of points in each bin is counted using b_n, if there is at least 1 empty bin exists for a component, that component is marked as a tree, otherwise as a pylon. Finally, for each pylon its location is obtained as the mean of its points.

3.2 Extraction of wires

In this step the non-vertical points are further processed to obtain the individual wires. In PLC object extraction it is hard to extract wire points as individual wire points due to their same linear properties. Thus, the following facts of overhead

PL structure are used: Wires do not intersect each other but maintain an adequate clearance to avoid unsafe contact themselves and they are hanged above the ground level at a certain height and carry the same direction in a span (Beaty , Fink). By using these characteristics a voxel traversing algorithm is developed to extract wire points into individual wires. Figure 1 shows the step for wire extraction. Figure 3 shows the wires in a span with their labels to illustrate the wire extraction algorithm. The detail of each step is given below:

1. Span Extraction: The transmission wires in a PLC is made up of numbers of segments (spans). These spans are connected to each other through pylons. Thus the extraction of individual pylons with their locations is helpful in determining these spans. Once pylons with their locations have been identified they are used to obtain the non-vertical points P_s for each span, i.e., points between two successive pylons in a corridor. The span extraction reduce the size of data points and makes the further processing of wire points easier.

2. Voxelization: The space between two pylons is divided into regular 3D grid. The 3D grid makes the processing complicated but unlike 2D grid it does not compromise on geometrical information of points in each grid cell (voxel). Each cuboid in a grid act as an individual voxel V. The size of V is kept to 0.5 m $\times$ 0.25 m $\times$ 0.25 m as the minimum gap between two
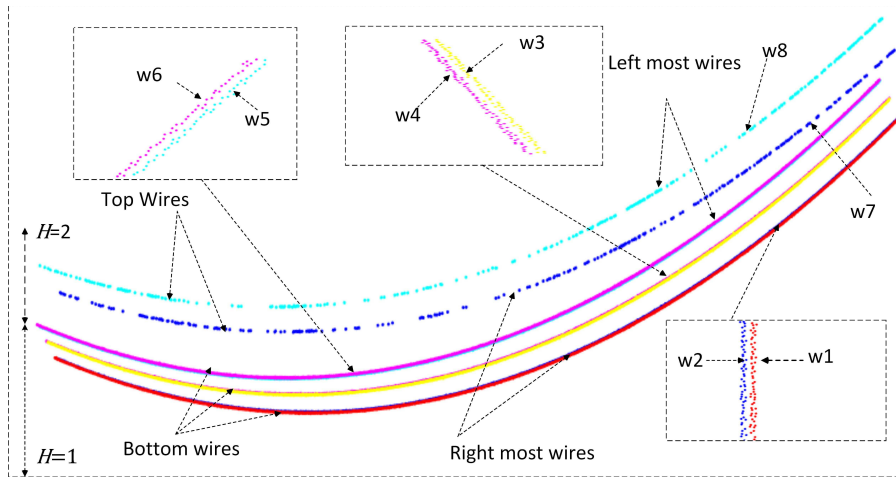
Figure 3. Wires labelling.

adjacent wires in the dataset is 0·5 m. The size of V is very important and derived through analysis of the input LiDAR points. This should be selected wisely as too small or big voxel size can give an inaccurate result. All voxels in a span are not occupied with points. The voxels between and outside the wire points are empty as all other objects are already removed earlier. Each V is given either of the two status by counting the number of points in it: Empty voxel V_E, if it does not have any points or one point, and occupied voxel V_O, if it has two or more points. The location of each V can be indexed by using the values row (i), column (j) and height (k). The maximum value of i, j and k are calculated as:

$$i = \lfloor \frac{(x_{max} - x_{min})}{l} \rfloor$$
$$j = \lfloor \frac{(y_{max} - y_{min})}{w} \rfloor \qquad (1)$$
$$k = \lfloor \frac{(z_{max} - z_{min})}{h} \rfloor$$

where $x_{max}, y_{max}, z_{max}$ = maximum coordinates of x, y, z
$x_{min}, y_{min}, z_{min}$ = minimum coordinates of x,y, z
l, w, h = length, width, height of voxel
i, j, k = location of voxel

3. Level of wires in span: The height (h) of points in each voxel with reference to ground is calculated and mean of height is allocated to corresponding V_O to check that all wires at at the same height or different. If all the wires have approximately same height (i.e., the difference of maximum height h_{max} and minimum height h_{min} is less then 1) the value of H will be set to 1 else set to 2. This value will be used in an algorithm to label wire points. The value of H can be calculated as :

$$H = \begin{cases} 1 & \text{if h is approximately same} \\ 2 & otherwise \end{cases} \qquad (2)$$

where h = minimum and maximum height difference in span
H= wire height levels

The value of H increases if height level of wires in PLC urges. The minimum value of H is 1, i.e., all the wires are hanged at
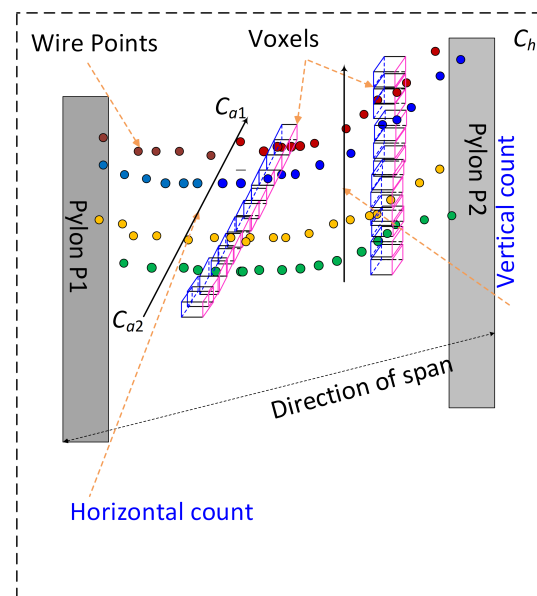

Figure 4. Feature extraction.

the same height. For the given sample scene the value of H is 2 (see Figure 3).

4. Horizontal count: For each V_O two numbers C_{a1} and C_{a2} expressing the count of V_E voxels on its both sides across the span are calculated. Figure 4 shows the directions to count these two values. This counting stops when a V_O voxel is found at the same height or the algorithm reaches the last voxel in the same direction. The value of C_{a2} is high and the value of C_{a1} is low for the right most (i.e., W_1 and W_7 wires see in Figure 3), while the value of C_{a1} is high and the value of C_{a2} is low for the left most wire (i.e., W_6 and W_8 wires in a Figure. 3).

5. Vertical count: For each V_O a height count C_h from the ground level in terms of V_E voxels in the height direction is calculated. Figure 4 shows the direction to count this value. The value of C_h will be high for top wires, e,g., wires W_7 and W_8 have high C_h values, then wires W_1 to W_6 in Figure 3.

6. Voxel Labelling: The V_O for which C_{a1}, C_{a2} and C_h values

neither heigh nor low will be considered in the next iteration for labelling. Thus, points in each voxels V_O are labelled according to the values of V_O by calculating range (R) using an equation given below.

$$R = [nl + 1, nl + 2H], \qquad (3)$$

where
$nl = 0$ in first iteration
and R is allocated to nl in next iteration

In every iteration the voxels with very high and low values will be labelled using a value of R. The value of C_{a1} is high and C_{a2} low for right most wire while the values are opposite for left most wires. So, in every iteration the left most and right most wires will be labelled. The thresholds in algorithm has been set representing the high and low values based on density of LiDAR point cloud data.

The voxel meeting the criteria will be labelled with values from R. The rest of the voxels will remain unlabelled and will be considered in the next iterations. This algorithm will proceed iteratively until all the V_O are labelled. This algorithm is efficient as only V_O and its neighbouring voxels are considered for labelling. The huge amount of empty voxels V_E are only counted for C_{a1}, C_{a2} and C_h. Finally, the voxels with the same labels are combined together to get the same wire points. The algorithm will do the extraction of wires in each span and will extract the individual wire points. Thus the wires are extracted in the form of segments of wire points. Once the extraction is accomplished the complete wire from PLC is formed by concatenated wire segments.

4. EXPERIMENTAL EVALUATION

This section is divided into four main sections. The brief overview on a dataset has been provided in section 3.1. Section 3.2 gives an overview on experiment set up. Section 3.3 presents the results and discussion on accuracy assessment of the PLC key objects extraction. Finally, the comparison of proposed method with the previous methods.

4.1 DATASET

Figure 5 shows the dataset from Maindample, Victoria, Australia. It is 5,560 m long and 330 m wide. The density of the input point cloud is 23.7 points/m^2. There are 2 transmission line corridors (TLCs) and one distribution line corridor (DLC). Each of the two TLCs has 13 pylons, so 26 in total. The only DLC is under the two TLCs and does not have enough points, therefore, excluded in this study. The total number of points in the dataset is 32,708,377, though the number of non-grounds is only 2,097,265 (16.5% of the total points). There are a total 14 spans in each TLC, where each span has eight wires at two height levels ($3 \times 2 + 2 \times 1$). The dataset also comes with a DTM (Digital Terrain Model) which is a 3D representation (x,y,z) of the earth surface and help to convert the individual input point height to the local ground height.

4.2 EXPERIMENT

The proposed method is implemented in MATLAB R2018b on Intel(R) Core(TM) on Intel(R) Core(TM) i7 CPU @ 2.70GHz processor and 16 GB RAM. Table 1 shows the summary of the ground truth used for evaluation of results. As the size of the
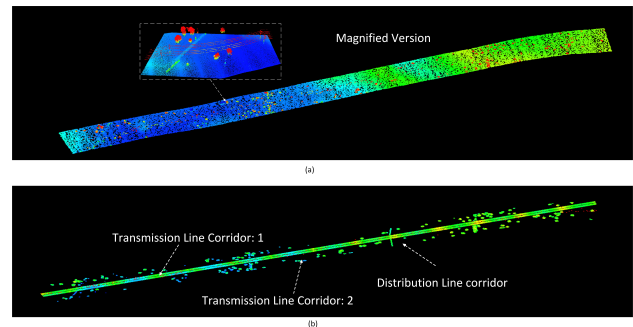

Figure 5. (a) Dataset with ground points, (b) Dataset without ground points.

dataset is very big so it is hard to collect ground truth for all points in the scene for evaluation. Only the first 6 spans of each of the two TLCs (total 12 spans out of 28) are used for evaluation of the proposed scheme. Points with height less than 1 m are not included in the ground truth data, as these points are assumed as terrain points. The number of wires in Table 1 is calculated by counting the number of wires in each span.

4.3 RESULTS AND DISCUSSIONS

For performance evaluation, object-based and point-based completeness C_m, correctness C_r and quality Q_l metrics are used and they are defined as follows (Wang et al., 2017):

$$C_m = \frac{TP}{TP + FN},$$
$$C_r = \frac{TP}{TP + FP}, \qquad (4)$$
$$Q_l = \frac{TP}{TP + FP + FN},$$

Where TP is truly detected pylons and wires for object-based evaluation and truly extracted pylon and wire points for point-based evaluation. FP is falsely detected wires and pylons and FN is pylons and wires which are not detected by the proposed method. Figure 6(a) shows the extracted pylon locations. These locations are used to find the wire points within spans. Figure 6(b) and (c) shows the extracted pylons and vegetation in TLC1 and TLC2. Figure 6(d) and (e) show the magnified version of an extracted pylon and a tree in a dataset.

For object-based evaluation, the total number of detected pylons and the total number of extracted wires in a dataset including the one in DLC are considered. Table 2 shows the object-based evaluation results for the dataset. All pylons in TLCs are detected except the ones which are located in the DLC. All the 224 wires in TLCs are extracted except the ones which are on the DLC. The object-based and point-based results are not provided for vegetation due to the absence of the ground truth for individual trees.

Pylons			Wires		
Comp.	Corr.	Qual.	Comp.	Corr.	Qual.
92.8	100	92	92.5	96	92.5

Table 2. Object-based evaluation on the whole dataset.

Sites	A	Points				Total		
	Area	All	Wire	Pylon	Trees	Span	Wires	Pylons
TLC 1	1,170 × 330	56,515	50,679	5,001	835	6	48	6
TLC 2	667 × 530	435,579	36,062	3,860	395,657	6	48	6
Total	1837×860	486,258	86,741	8,861	396,492	12	96	12

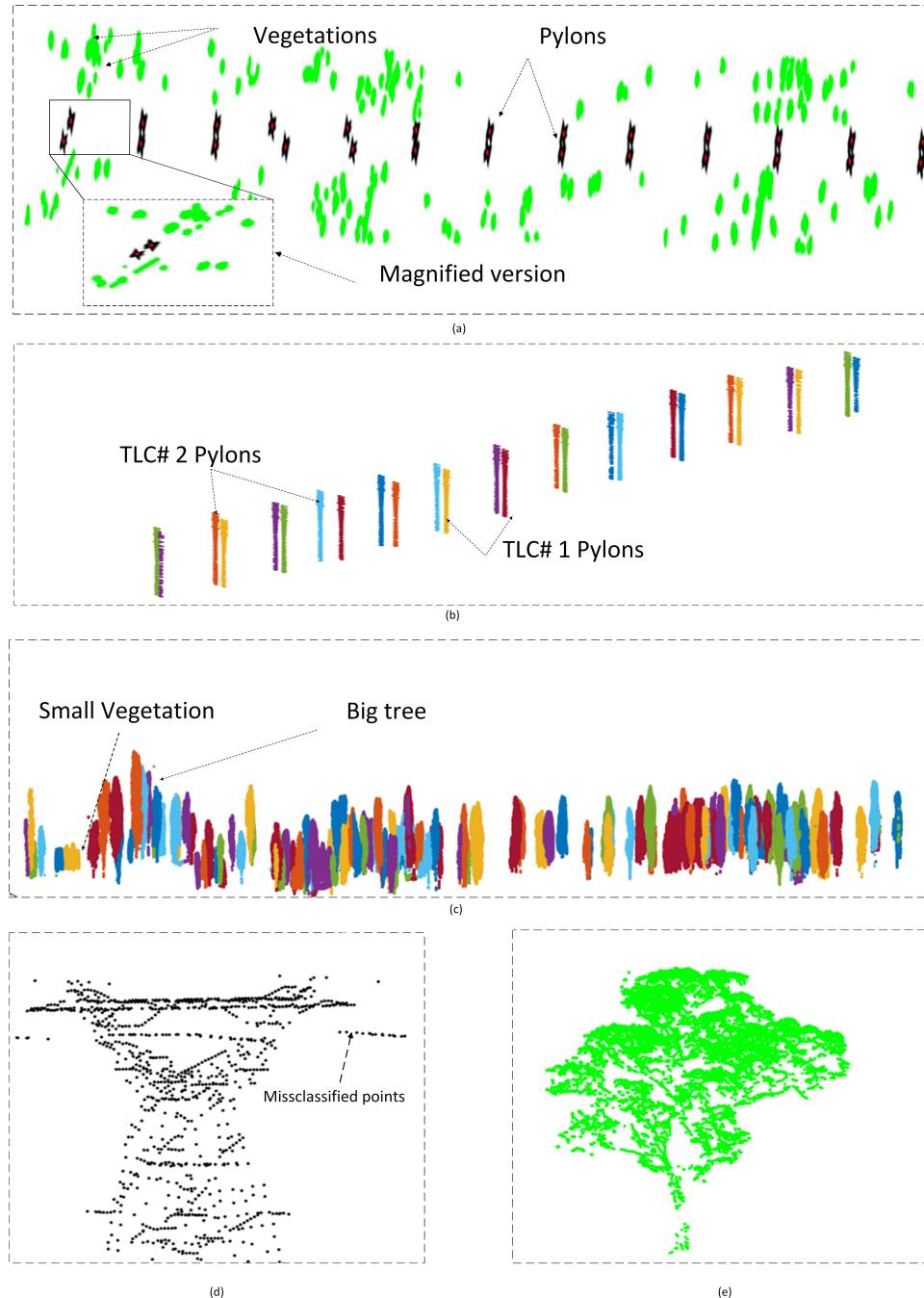Table 1. Summary of the two ground truth sites.

Figure 6. (a) Pylon locations, (b) Extracted pylons, (c) Extracted vegetation, (d) Individual pylon, (e) Individual tree.

Table 3 shows point-based evaluation for wire and pylon points. In both sites, some of the wire points are misclassified as pylon points (see Figure. 6(d)) as these wire points are very close to pylons and hard to separate using vertical profile features. Localisation error of pylon locations is also calculated by estimating the difference between the two mean points of the extracted pylon and corresponding ground truth pylon data. Figures 7(a) and (b) show the extracted wires in both corridors. There are some errors in detecting PL points in adjacent wires see Figure 7(b). This is due to the fact that the points of adjacent wires are very close to each other. A voxel can have points from two adjacent wires in that case some of the the

TLC	Wires			Pylons				
	Comp.	Corr.	Qual.	Comp.	Corr.	Qual.	2D error.	3D error.
TLC 1	97.7	98.6	98.4	98.9	99.8	99.7	0.19	0.34
TLC 2	98.1	99.2	98.63	98.5	99.7	99.6	0.06	0.28
Average	97.9	98.9	97.015	99.9	99.75	99.65	0.12	0.31

Table 3. point-based evaluation on the dataset.
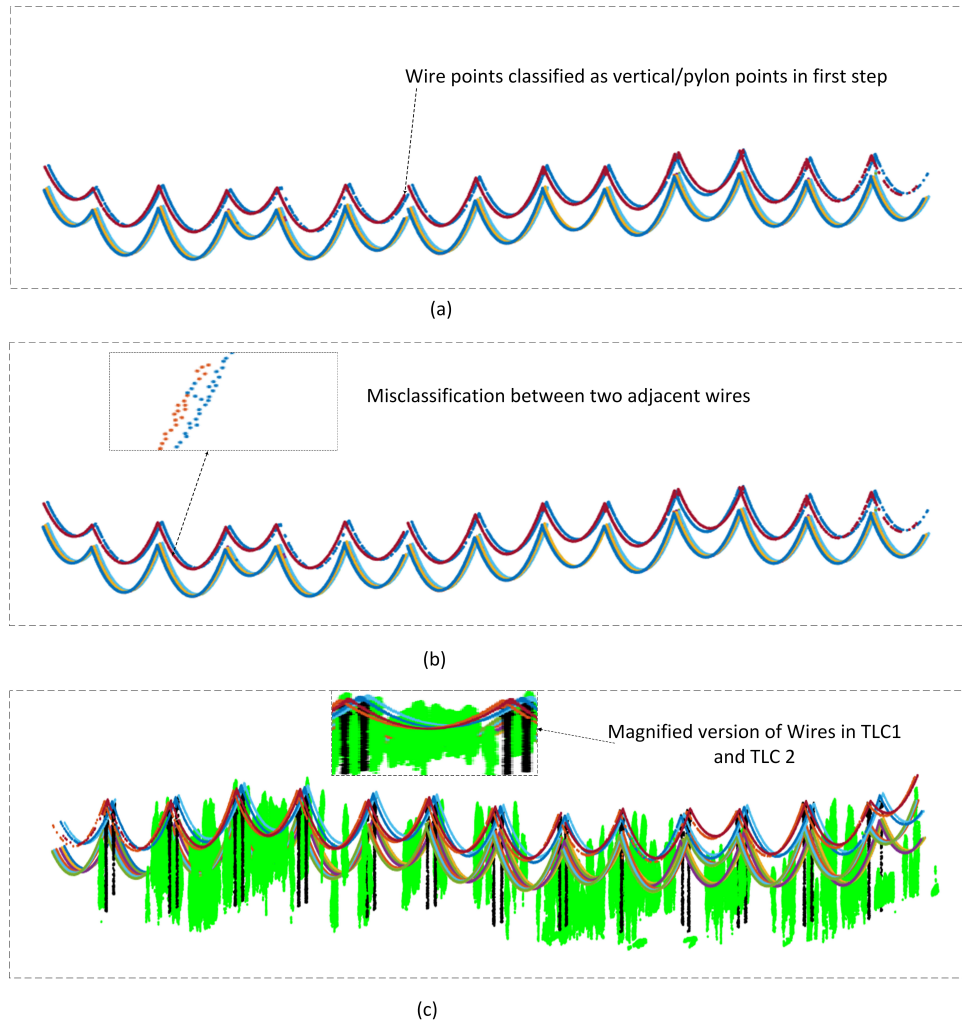

(a)

(b)

(c)

Figure 7. (a) Extracted wires in TLC 1, (b) Extracted wires in TLC 2, (c) Extracted wires, pylons and vegetation points.

points may be wrongly misclassified. Though there is no wrong classification of PL points which are not in adjacent wires. Also, some of the points may be misclassified as pylon points as they may be very close to pylons and are not extracted as wire points in the first step see Figure 6(d).

Step	Section	Time(mins.)
Removal of ground points	3.1	1.2
VPF feature calculation	3.1	2.3
Final Pylons and trees	3.1	3.4
Wire extraction(each span)	3.2	2.5

Table 4. Running time for different steps of the proposed method.

Table 5 shows the running time for different steps of the proposed method when it is applied to the large dataset (5,560 m × 330 m) with more than 32.5 million points in the input point cloud data. For each step in the table the fastest time is recorded from about ten runs. The time is proportional to the size of dataset and the size of each span.

4.4 Comparison with existing methods

The novelty of this study is the individual wire extraction, where the previous studies mostly focused on classification of wires as a whole class. Where (Kim and Sohn, 2010) (Guo et al., 2015) (Wang et al., 2017) offered point- based accuracy of

with 97.33% 93.4% 98% respectively. The proposed method provide 98.9% correctness for the extracted wire points.

Only few studies have given an automated solution for individual PL extraction in which they had presented results in few spans and didn't extract the complete wire from PLC. such as a method in (Jwa et al., 2009) is based on automated voxle-based solution for PL extraction and reconstruction with completeness of 93.4%. (Cheng et al., 2014) proposed a method to extract PLS from Urban areas using vehicle-borne LiDAR data with correctness and completeness of 100% and 97.2% respectively. The proposed method has achieved better accuracy i.e., 98% and 99% in terms of completeness and correctness. Moreover, we have used 2 corridors, while each corridor has 14 spans to do the evaluation of proposed method. However the proposed algorithm may give less accurate results in the case of occlusion and noisy wires occlusion. In that case pre-processing steps, will be required to remove the noise to perform the voxel-based extraction.

5. CONCLUSION

In this work, we have addressed the issue of extraction of individual pylons and wires which are very important for modelling of 3D objects in a power line corridor (PLC) map. Existing methods mostly classify points into distinct classes like pylons and wires, but hardly into individual pylons or wires. The extraction of individual objects is important for a detailed PLC mapping.

To overcome the above mentioned shortcomings this paper proposes a framework that combines the supervised and unsupervised methods to extract individual PLC objects. A voxel-based algorithm is developed to do an extraction of individual wires by using the PL characteristics. The proposed method shows 98% and 99% completeness and correctness for pylons and wires respectively. In future, we will investigate the modelling of wire points using the catenary curve equation and will perform the extraction of PLC objects in more complex datasets which have occluded and noisy wires. Also, the location of pylons, wires and vegetation can be further used to monitor the vegetation near PLC to prevent the risk from tall and growing trees closely to power lines.

References

Awrangjeb, M., Jonas, D., Zhou, J., 2017. An automatic technique for power line pylon detection from point cloud data. *2017 International Conference on Digital Image Computing: Techniques and Applications (DICTA)*, IEEE, 1–8.

Axelsson, P., 1999. Processing of laser scanner data—algorithms and applications. *ISPRS Journal of Photogrammetry and Remote Sensing*, 54, 138–147.

Beaty, H., Fink, D., 2007. *Standard handbook for electrical engineers*. McGraw-Hill New York.

Cheng, L., Tong, L., Wang, Y., Li, M., 2014. Extraction of urban power lines from vehicle-borne LiDAR data. *Remote Sensing*, 6, 3302–3320.

n.d.

Guo, B., Huang, X., Zhang, F., Sohn, G., 2015. Classification of airborne laser scanning data using JointBoost. *ISPRS Journal of Photogrammetry and Remote Sensing*, 100, 71–83.

Jwa, Y., Sohn, G., Kim, HB., 2009. Automatic 3d powerline reconstruction using airborne lidar data. *Int. Arch. Photogramm. Remote Sens*, 38, W8.

Kim, H., Sohn, G., 2010. 3D classification of power-line scene from airborne laser scanning data using random forests. *Int. Arch. Photogramm. Remote Sens*, 38, 126–132.

Matikainen, L., Lehtomäki, M., Ahokas, E., Hyyppä, J., Karjalainen, M., Jaakkola, A., Kukko, A., Heinonen, T., 2016. Remote sensing methods for power line corridor surveys. *ISPRS Journal of Photogrammetry and Remote Sensing*, 119, 10–31.

McLaughlin, R., 2006. Extracting transmission lines from airborne LIDAR data. *IEEE Geoscience and Remote Sensing Letters*, 3, 222–226.

Sohn, G., Jwa, Y., Kim, H., 2012. Automatic powerline scene classification and reconstruction using airborne lidar data. *ISPRS Ann. Photogramm. Remote Sens. Spat. Inf. Sci*, 13, 28.

Wang, Y., Chen, Q., Liu, L., Zheng, D., Li, Chaokui, L., Kai, 2017. Supervised classification of power lines from airborne LiDAR data in urban areas. *Remote Sensing*, 9, 771.

Zhu, L., Hyyppä J., 2014. Fully-automated power line extraction from airborne laser scanning point clouds in forest areas. *Remote Sensing*, 6, 11267–11282.